University of Montana
ScholarWorks at University of Montana

Undergraduate Theses, Professional Papers, and Capstone Artifacts

2021

Introducing human-like mutations in yeast iso-1-cytochrome c to decrease peroxidase activity in apoptosis

Sidney L. Thompson
st248129@umconnect.umt.edu

Follow this and additional works at: https://scholarworks.umt.edu/utpp
Let us know how access to this document benefits you.

Recommended Citation
Thompson, Sidney L., "Introducing human-like mutations in yeast iso-1-cytochrome c to decrease peroxidase activity in apoptosis" (2021). *Undergraduate Theses, Professional Papers, and Capstone Artifacts*. 341.
https://scholarworks.umt.edu/utpp/341

This Thesis is brought to you for free and open access by ScholarWorks at University of Montana. It has been accepted for inclusion in Undergraduate Theses, Professional Papers, and Capstone Artifacts by an authorized administrator of ScholarWorks at University of Montana. For more information, please contact scholarworks@mso.umt.edu.

Introducing human-like mutations in yeast iso-1-cytochrome c to decrease peroxidase activity in apoptosis

Sidney L. Thompson

Submitted in partial fulfillment of the requirements of the Davidson Honors College

University of Montana

April, 2021

Faculty Advisor:
Professor Bruce E. Bowler
Chemistry and Biochemistry

Graduate Mentor:
Ariel K. Frederick
Biochemistry and Biophysics Graduate Program

Abstract: The mitochondria is an important organelle for a large assortment of metabolic processes. Cytochrome *c* (Cyt*c*), a vital protein found in the mitochondria, is critical for life and death processes in eukaryotic cells. One of these functions includes shuttling electrons through the electron transport chain during cellular respiration. Cyt*c* is also an essential signaling protein in the pathway of apoptosis, also known as programmed cell death. Yeast has similar components of this cell death pathway to higher eukaryotes such as humans, but does not contain all of the same optimized cascade processes. Additionally, the peroxidase activity, an early signal in the apoptotic pathway, is much lower in human Cyt*c* when compared to wild type yeast iso-1-Cyt*c*. This suggests the evolution of an optimized "off" state in the peroxidase activity of human Cyt*c*. In the least stable substructures of Cyt*c*, which mediate peroxidase activity, three amino acid sites co-evolve between human Cyt*c* and iso-1-Cyt*c*. In comparison to iso-1-Cyt*c*, human Cyt*c* contains the substitutions S40T, V57I and N63T. These should stabilize this hydrophobic interface in human Cyt*c* by the addition of a methyl group in each substitution when compared to iso-1-Cyt*c*. All possible single, double and triple substitution variants from Hu Cyt*c* were introduced into iso-1-Cyt*c* to test the hypothesis that they would increase the stability of iso-1-Cyt*c,* causing the peroxidase activity of iso-1-Cyt*c* to decrease. Bacterial protein expression of the single and double mutation variants in BL21 *Escherichia coli* cells, followed by protein purification were performed. Further experimentation on the individual mutant proteins, to test the hypothesis, included measurement of peroxidase activity, the alkaline transition, and protein stability. Overall we find only moderate effects on global and local stability by each of the variants introduced. While there are minor changes in the K_M for each of the variants in comparison to WT, k_{cat} shows more variation between WT and variants at increasing pH values. These findings suggest that these variants evolved to preserve rather than change function.

Introduction

Mitochondrial cytochrome *c* (Cyt*c*) has important functions as an electron carrier in the electron transport chain during cellular respiration.[4] Cyt*c* has more recently been found to function as a signaling agent in the intrinsic pathway of apoptosis where it has an important role in forming the apoptosome, which activates caspase-9, ultimately initiating the point of no return signaling for cell death. Under apoptotic conditions, peroxidation of cardiolipin (CL) by Cyt*c* may occur, causing dissociation of membrane-bound Cyt*c*, facilitating its release into the cytoplasm.[5] This process allows free Cyt*c* to bind to apoptotic protease-activating factor 1 to form the apoptosome.

Yeast does not contain the same components of this apoptotic pathway found in human Cyt*c*.[3] In comparison to human, yeast has Cyt*c* with a 20-fold higher intrinsic peroxidase activity, suggesting that Cyt*c* in higher eukaryotes has evolved an "off" switch in the intrinsic apoptotic pathway in order to limit its peroxidase activity. Past studies have identified naturally occurring variants of human Cyt*c* related to thrombocytopenia, which have shown both higher intrinsic peroxidase activity as well as higher apoptotic activity.[1,8,9,10]

In order for Cyt*c* to produce higher peroxidase activity it must contain an open coordination site. This requires Cyt*c* to undergo a conformational change to free the coordination site from its natural hexa-coordinated heme conformation. Ω-loop C and D have been implicated in providing access to these peroxidase conformers by the loss of Met80 ligation to the heme. This occurs from modest structural rearrangement of these least stable structures in Cyt*c*. Recent research has directed focus to Ω-loop C as the key substructure of Cyt*c* to provide access to the peroxidase competent conformer of Cyt*c*. Naturally occurring variants located in Ω-loop C of human Cyt*c* linked to thrombocytopenia and having increased peroxidase activity have been

identified.[1,8,9,10] However, as Ω-loop C is more poorly conserved when compared to Ω-loop D,[6,7] defining which of its residues have evolved the "off" state of the peroxidase activity is not straightforward. S40T, V57I, and N63T substitutions occur in human Cyt*c* relative to yeast iso-1-Cyt*c*.[2] These co-varying residues[2] have been found to form a hydrophobic cluster at the interface of Ω-loop C and D and the 60s helix in human Cyt*c* (Figure 1). The human variants add a methyl group to the hydrophobic cluster, which is thought to stabilize this interface.

All possible single, double and triple substitution variants from Hu Cyt*c* were introduced into iso-1-Cyt*c* to test the hypothesis that they would increase the stability of iso-1-Cyt*c,* causing the peroxidase activity of iso-1-Cyt*c* to decrease. Bacterial protein expression of the single and double mutation variants in BL21 *Escherichia coli* cells, followed by protein purification were performed. Further experimentation on the individual mutant proteins to test the hypothesis included measurement of peroxidase activity, the alkaline transition, and protein stability. Overall we find only moderate effects on global and local stability by each of the variants introduced. While there are minor changes in the K_M for each of the variants in comparison to WT, k_{cat} shows more variation between WT and variants at increasing pH values. These findings suggest that sequence positions 40, 57 and 63 evolved to preserve rather than change function.

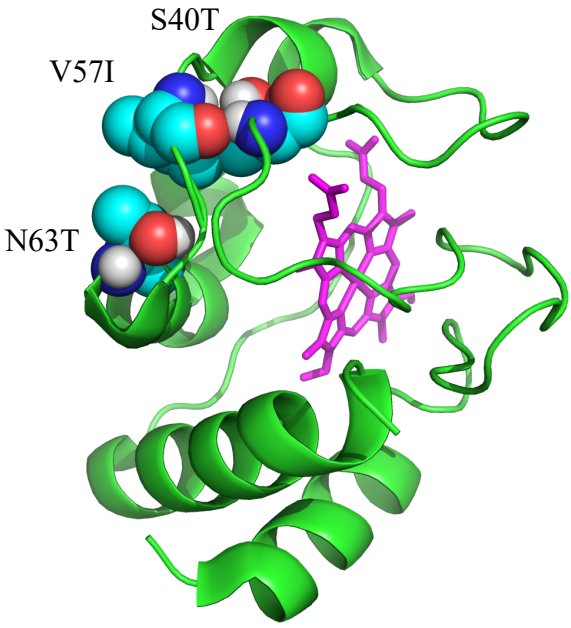

Figure 1. Structure of human cytochrome *c* (PDB:3ZCF)[1] with relevant variant residue sites highlighted at 40, 57, and 63 to display the hydrophobic cluster formed by the co-varying residues at the interface of Ω-loops C, D and the 60s helix.

Materials and Methods

Mutagenesis and protein purification

Variants used in this work were prepared in the laboratory course BCH 486 under the guidance of Professor Bowler or by Ariel Frederick using PCR-based site-directed mutagenesis. All mutations were confirmed by dideoxy sequencing (Eurofins Genomics). dsDNA (pRbs_BTR1 vector[12]) carrying the S40T, N63T, V57I, and S40T/N63T variants of yeast iso-1-Cyt*c* were transformed into competent BL21(DE3) E. *coli* cells. All transformants plated on L-ampicillin agar and incubated overnight at 37°C were suspended in sterile L-broth and used to inoculate 6 L of YT media with 1.0 mL of 100 mg/mL ampicillin in each liter of media. Cultures were incubated at 37°C and with shaking at 150 rpm for approximately 30-36 hours in the shaker incubator. The cells were harvested by centrifugation and frozen at -80°C. Cells were suspended in lysis buffer (100 mM Tris, 500 mM NaCl, 1 mM EDTA pH 8.0; a few crystals of DNAse and

RNAse and 2 mM PMSF) using 5-10 mL/mg of cells, followed by stirring for 1 hour at 0°C. The cells were broken using a Q700 sonicator (Qsonica, LLC), and the lysate was cleared by centrifugation. The supernatant was 50% saturated by ammonium sulfate, stirred overnight (approximately 16 hours) and precipitates were removed by centrifugation. The collected supernatant was placed in dialysis tubing and dialyzed against 12.5 mM sodium phosphate, pH 7.2, 1 mM EDTA, and 2 mM β-mercaptoethanol (β-ME) buffer stirring for approximately 24 hours at 0°C. The buffer was reprepared and replaced, dialyzing the protein a second time for 24 hours. The protein was then absorbed to CM-Sepharose fast flow resin (100 mL) overnight, then placed in a glass column draining excess liquid. The resin was equilibrated in 50 mM sodium phosphate buffer, pH 7.2, 1 mM EDTA, 2 mM β-ME for 30 minutes and the protein eluted with a linear gradient of 0-0.8 M NaCl in 50 mM sodium phosphate buffer, pH 7.2, 1 mM EDTA, 2 mM β-ME. After concentration and exchange into Milli-Q water three times by ultrafiltration the protein was frozen and stored at -80°C. Before experimentation, protein samples were reduced with sodium dithionite ($Na_2S_2O_4$) and purified using a HiTrap SP HP 5.0 mL column coupled to an AKTAprime plus chromatography system (GE Healthcare Life Sciences). A gradient from 0 – 60% B over a volume of 60 mL at a flow rate of 1 mL/min was used for protein elution. Protein samples were concentrated by ultrafiltration and oxidized with $K_3[Fe(CN)_6]$. Oxidized Cyt*c* was separated from the oxidizing agent by Sephadex G25 chromatography using a running buffer specific to the planned experiment.

Global stability measurements by guanidine hydrochloride denaturation

Global stability measurements were made using GdnHCl as a denaturant. GdnHCl unfolding was monitored at 25°C with an Applied Photophysics Chirascan circular dichroism

spectrometer coupled to a Hamilton M635 automated titrator. A solution of 4 μM S40T/N63T variant in 20 mM Tris, pH 7.5, 40 mM NaCl was titrated with ~6 M GdnHCl containing the S40T/N63T variant at the same concentration in 20 mM Tris, pH 7.5, 40 mM NaCl in a 10 mm pathlength cuvette containing a stir bar. After each addition by the titrator, the sample was stirred to mix for 300 seconds, and allowed to settle for 20 seconds while data were collected at 222 (α-helix) and 250 nm. Baseline correction was accomplished by subtracting the ellipticity at 250 nm from the ellipticity at 222 nm ($\theta_{222corr} = \theta_{222} - \theta_{250}$). Using SigmaPlot (Systat Software), $\theta_{222corr}$ was plotted against GdnHCl concentration for the S40T/N63T variant and fit to a two-state model using nonlinear-least squares methods, assuming a linear free energy relationship (Eq. 1) and a native state baseline that is independent of GdnHCl concentration (Eq. 2).

$$(1)\ \Delta G_u = \Delta G_u^{\circ\prime}(H_2O) - m[\mathrm{GdnHCl}]$$

$$(2)\quad \theta_{222corr} = \frac{\left[(\theta_N)+(\theta_D+m_D[\mathrm{GdnHCl}])\cdot\exp\left\{\frac{m[\mathrm{GdnHCl}]-\Delta G_u^{\circ\prime}(H_2O)}{RT}\right\}\right]}{1+\exp\left[\frac{m[\mathrm{GdnHCl}]-\Delta G_u^{\circ\prime}(H_2O)}{RT}\right]}$$

In Eq. 1, $\Delta G_u^{\circ\prime}(H_2O)$ is free energy unfolding in the absence of denaturant, and *m* is the rate of change of free energy with respect to GdnHCl concentration (the *m*-value). $\Delta G_u^{\circ\prime}(H_2O)$ and the *m*-value were extracted from fits of the data to Eq. 2. In Eq. 2 θ_N is the native baseline and θ_D and m_D are the intercept and slope of the denatured state baseline. The parameters from fits to three independent trials were averaged, and the error was calculated based on the standard deviation of the average.

Measurement of the alkaline conformational transition

For the alkaline transition measurements, a Beckman Coulter DU 800 Spectrophotometer was used to monitor pH transitions at 695 nm. 200mM NaCl running buffer was used in a Sephadex G25 chromatography separation of the oxidized protein. The collected oxidized

protein was concentrated by ultrafiltration using centrifugation at 4500 rpm for approximately 5 minutes. Concentration and degree of oxidation of the protein were evaluated by UV-Vis spectroscopy. The amount of dilution of the protein in the solution was determined based on the initial concentration. A 1000 μL solution of 200 μM oxidized S40T/N63T variant in 200 mM NaCl was prepared for the 2X stock solution. The 2X S40T/N63T stock solution and Milli-Q water were mixed 1:1 to produce the 1X solution of 100 μM oxidized S40T/N63T in 100 mM NaCl. pH titrations were carried out by adding either NaOH or HCl solutions to the 1X solution for the appropriate pH increments with the overall data ranging from approximately pH 6 to pH 10. Equal volumes of the 2X S40T/N63T stock solution were added to maintain a constant protein concentration throughout the titration. pH measurements were made with each protein and NaOH/HCl solution addition using a Denver Instrument UB-10 pH/mV meter and an Accumet double junction semi-micro pH probe. The absorbance at 750 nm was subtracted from the absorbance at 695 nm to correct for baseline drift ($A_{695corr} = A_{695} - A_{750}$). The plots of $A_{695corr}$ versus pH for S40T/N63T were fit to the modified Henderson – Hasselbalch equation, Eq. 3.

$$A_{695\text{corr}} = \frac{A_{\text{N}} + A_{\text{Alk}} \times 10^{n[\text{p}K_{\text{app}} - \text{pH}]}}{1 + 10^{n[\text{p}K_{\text{app}} - \text{pH}]}} \quad (3)$$

For Eq. 3, A_N is the corrected absorbance for the native state with Met80 bound to the heme at 695 nm, A_{alk} is the corrected absorbance for the alkaline state at 695 nm with Lys72, Lys73, or Lys79 as the alkaline state heme ligand, pK_{app} is the apparent pK_a of the alkaline transition, and n is the number of protons connected to the alkaline transition.

Guaiacol assay of peroxidase activity

Peroxidase activity was measured using guaiacol and monitored with an Applied Photophysics SX20 stopped-flow apparatus. The formation of tetraguaiacol from guaiacol and H_2O_2 in the presence of Cyt*c* was measured at 470 nm. Solutions of 4 μM Cyt*c*, 100 mM H_2O_2, and 400 μM guaiacol were made using the specific pH buffer indicated for the trial. The buffers used were 50 mM sodium acetate (pH 5.0) MES (pH 6.0-6.5), NaH_2PO_4 (pH 6.75-7.5), and Tris (pH 7.75-8.75). Concentrations were determined using the extinction coefficient of H_2O_2 (ε_{240} = 41.5 M^{-1} cm^{-1}) and guaiacol (ε_{274} = 2150 M^{-1} cm^{-1}). 4X Cyt*c* and 4X guaiacol solutions in 50 mM buffer were mixed 1:1 to produce a 2X Cyt*c* 2X guaiacol stock in 50 mM buffer. This 2X stock solution was mixed 1:1 with 100mM H_2O_2 in 50 mM buffer with the stopped flow instrument, yielding a final solution containing 1 μM Cyt*c,* 50 mM H_2O_2 and guaiacol at the desired concentration in 50 mM buffer. Final concentrations of guaiacol after mixing were 0, 2, 4, 6, 8, 10, 15, 20, 25, 30, 40, 50, 60, 80, and 100 μM.

A_{470} versus time data were plotted and the segment of the plot with the greatest slope following the initial lag phase was used to obtain the initial velocity, v, at each guaiacol concentration. The data were fit to a linear equation and the slope from the five repeats was averaged. The slope was divided by the extinction coefficient of tetraguaiacol at 470 nm (ε_{470} = 26.6 mM^{-1} cm^{-1}) and multiplied by 4 (4 guaiacol consumed per tetraguaiacol produced) to give the initial rate of guaiacol consumption, v. The initial rate, v, was divided by iso-1-Cyt*c* concentration, plotted against guaiacol concentration and fit to the Michalis-Menten Eq. 4 to obtain K_m and k_{cat} values.

$$(4) \quad \frac{v}{[\text{iso}-1-\text{Cyt}c]} = \frac{k_{\text{cat}} \bullet [\text{Guaiacol}]}{K_{\text{m}} + [\text{Guaiacol}]}$$

Results

The data shown in the figures in each section is for the S40T/N63T variant, which was collected and analyzed by the author of this report. Thermodynamic and peroxidase activity parameters for other variants were collected and analyzed by graduate mentor Ariel Frederick and are presented to provide context for the results obtained with the S40T/N63T variant.

Global stability of iso-1-Cytc variants

The global unfolding thermodynamics of the S40T, N63T, V57I, S40T/N63T, S40T/V57I, N63T/V57I and S40T/V57I/N63T iso-1-Cyt*c* variants was monitored by circular dichroism spectroscopy using GdnHCl as a denaturant. Figure 2 shows the $\theta_{222corr}$ versus GdnHCl concentration denaturation curve of the S40T/N63T variant. Similar data were obtained for each of the variants. Thermodynamic parameters for each of the variants are given in Table 1. As seen by the midpoint GdnHCl concentration for unfolding, C_m, the GdnHCl *m*-value, and ΔG in Table 1, each of the single and double mutation variants have moderate effects on global stability when compared to WT iso-1-cytochrome *c*.

Table 1. Thermodynamic parameters for global unfolding of WT and each of the variants of iso-1-Cyt*c*

Variant	ΔG, kcal mol^{-1}	m, kcal mol^{-1} M^{-1}	C_m, M
WT	5.05 ± 0.30	4.24 ± 0.13	1.19 ± 0.04
S40T	4.99 ± 0.09	3.94 ± 0.16	1.27 ± 0.03
N63T	5.38 ± 0.12	4.01 ± 0.10	1.34 ± 0.01
V57I	4.22 ± 0.13	3.54 ± 0.12	1.19 ± 0.01
N63T/V57I	5.40 ± 0.16	3.87 ± 0.12	1.40 ± 0.03
S40T/V57I	4.23 ± 0.07	3.66 ± 0.22	1.16 ± 0.06
S40T/N63T	4.50 ± 0.12	3.85 ± 0.07	1.17 ± 0.01
S40T/V57I/N63T	4.197 ± 0.004	3.49 ± 0.05	1.20 ± 0.02

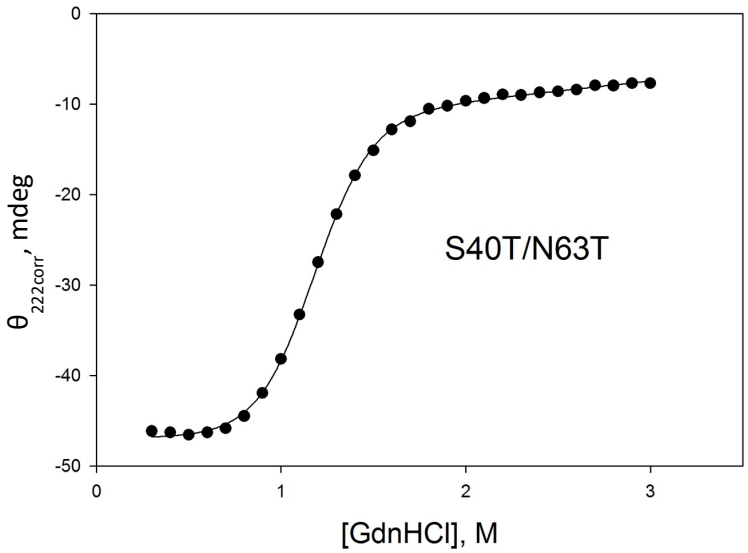

Figure 2. Denaturation curve of S40T/N63T of $\theta_{222corr}$ vs concentration of GdnHCl. Parameters obtained from the fits are given in Table 1. Experiments were performed at 25°C in 20mM Tris, 40mM NaCl, pH 7.5 at 4uM S40T/N63T protein concentration.

Local unfolding via the alkaline conformational transition

The local unfolding thermodynamics for the alkaline conformational transition of the S40T, N63T, V57I, S40T/N63T, S40T/V57I, N63T/V57I, and S40T/V57I/N63T variants were determined by pH titration monitored by the loss of the 695 nm band, following the loss of Met80-heme ligation as shown for the S40T/N63T variant in Figure 3. As shown in Table 2, the number of protons involved in this transition is approximately equal to 1 for WT and each of the iso-1-Cyt*c* variants. The apparent pKa values, $pK_{app,}$ for the N63T/V57I and S40T/N63T variants have small decreases of 0.2-0.4 units compared to WT, and the V57I variant has a small increase of 0.1-0.2 units compared to WT. The remaining single mutation variants, S40T, N63T, and V57I, as well as S40T/V57I and S40T/V57I/N63T are similar in value to the pK_{app} of WT iso-1-Cytc (Table 2). Overall, these variants have only moderate effects on the pK_{app} value when compared to WT.

Table 2: Thermodynamic parameters for the alkaline transition of WT and iso-1-Cytc c variants.

Variant	pK_{app}	n
WT	8.00 ± 0.05	0.98 ± 0.01
V57I	8.17 ± 0.06	1.13 ± 0.12
S40T	7.99 ± 0.06	0.98 ± 0.17
N63T	8.01 ± 0.05	0.95 ± 0.06
N63T/V57I	7.64 ± 0.04	0.96 ± 0.05
S40T/V57I	7.94 ± 0.16	1.05 ± 0.13
S40T/N63T	7.84 ± 0.11	0.98 ± 0.12
S40T/V57I/N63T	7.96 ± 0.10	0.89 ± 0.08

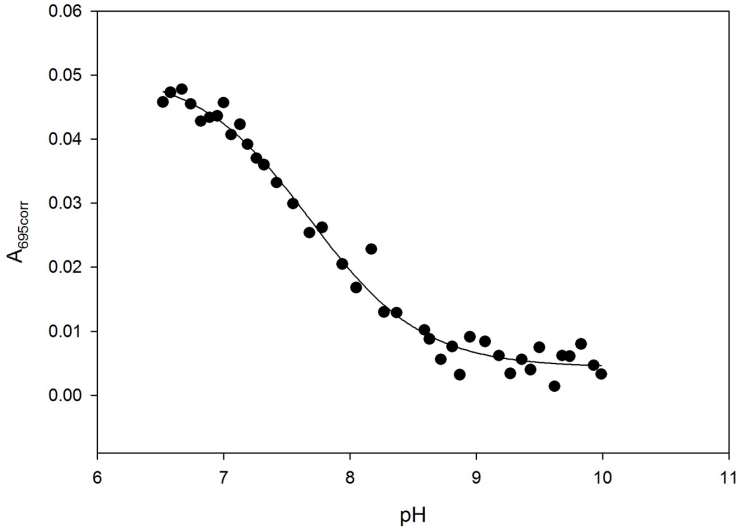

Figure 3. Plot of $A_{695corr}$ vs pH for the alkaline transition of S40T/N63T iso-1-Cyt*c.* Equation 1 from the Methods section was fit to the plot in order to determine the thermodynamic parameters pK_{app} and n of the alkaline transition in Table 1.

Peroxidase activity of WT and iso-1-Cytc variants

Peroxidase activity of WT and the iso-1-Cytc variants S40T, N63T, V57I, S40T/N63T, N63T/V57I, S40T/V57I, and S40T/V57I/N63T was measured by monitoring the formation of tetraguaiacol from guaiacol in the presence of H_2O_2. The Michaelis-Menten equation fit to the guaiacol concentration plots was used to determine the k_{cat} and K_m for pH 5, 6, 7, and 8. An example plot for S40T/N63T at pH 7 is shown in Figure 4. As shown in Figure 5, peroxidase assays indicate minimal effects of all variants on K_m compared to WT iso-1-Cyt*c*. Figure 6 shows that at pH 5 the k_{cat} for each variant is similar to the k_{cat} value for WT. As pH increases from 5 to 8, the k_{cat} value for each variant appears to decrease in comparison to WT.

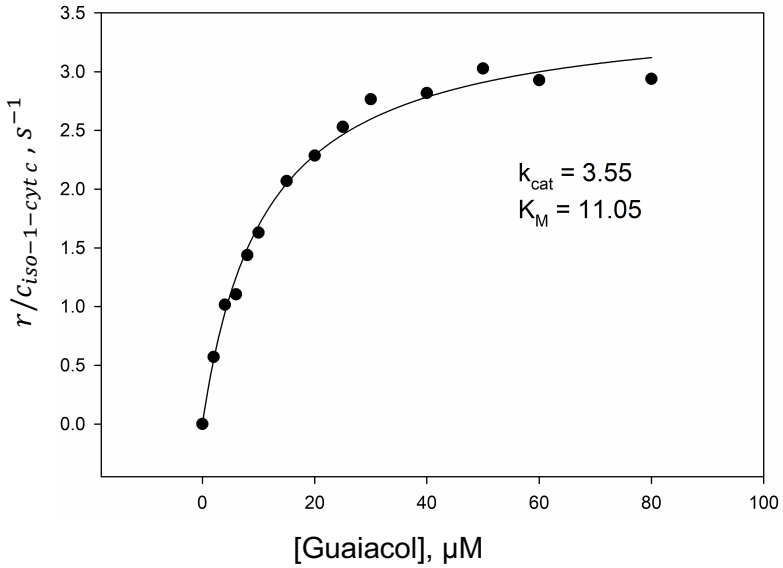

Figure 4. Peroxidase assay guaiacol concentration plot of S40T/N63T iso-1-Cyt*c* variant at pH 7 fit to the Michaelis-Menten equation to determine K_M and k_{cat} values.

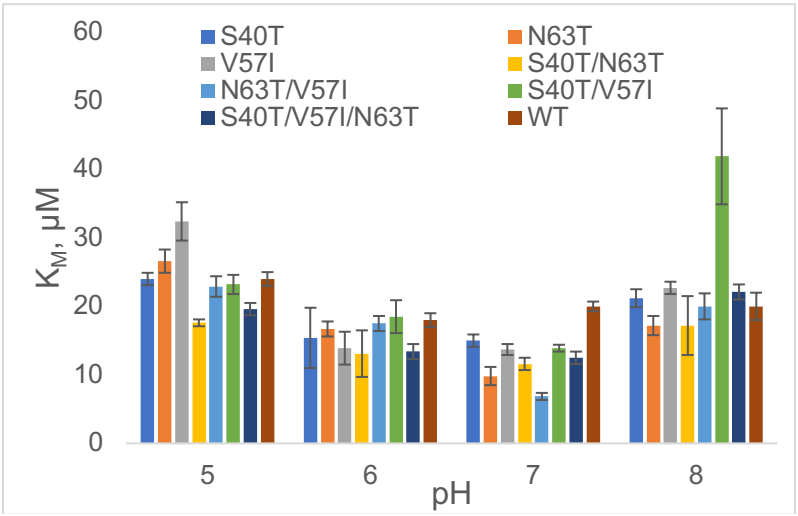

Figure 5. K_m values at pH 5-8 for WT and all iso-1-Cyt*c* variants.

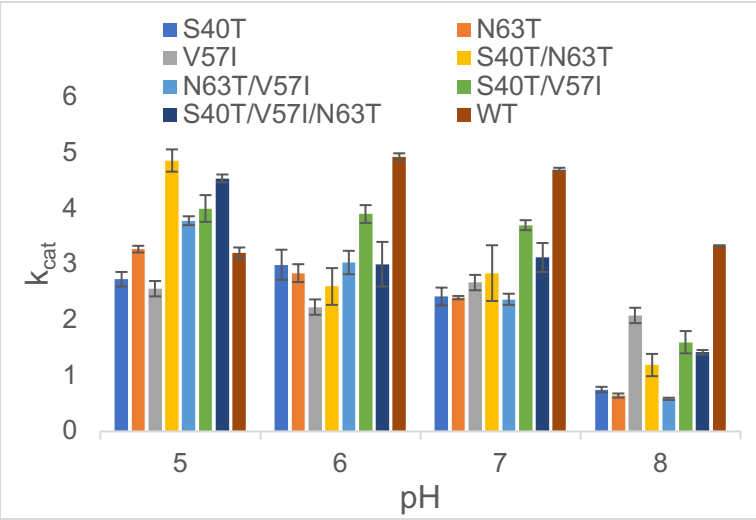

Figure 6. k_{cat} values at pH 5-8 for WT and all iso-1-Cyt*c* variants.

Discussion

The effects of each of the variants on global stability of iso-1-Cyt*c* are relatively modest (Table 1). All variants have reduced m-values compared to WT. The triple mutant variant has an m-value similar in value to human Cyt*c* (3.5-3.7 kcal mol^{-1} M^{-1}).[11] This indicates that the variants, specifically V57I, may control cooperativity of unfolding. The local stability, was measured by the alkaline conformational transition, pK_{app}. The local stability of V57I, N63T/V57I, and S40T/N63T show the most variation from yeast iso-1-Cytc WT, with a 0.1-0.2 unit increase in value for V57I and 0.2-0.4 decrease in value for the N63T/V57I and S40T/N63T. The remaining single, double, and triple mutation variant effects on local stability are relatively modest and within error limits of yeast iso-1-Cyt*c* WT. Given that pK_{app} is believed to reflect the local stability of Ω-loop D, the variants are compensatory overall, suggesting that the variants have evolved to maintain the local stability of Ω-loops C and D.

The implication of each of the variants for the intrinsic peroxidase of Cyt*c* as it relates to apoptosis was also determined. Peroxidase assays indicate minimal effects of all variants on K_M compared to WT iso-1-Cyt*c* (Figure 5). Overall, the single mutations appear to have the greatest

variation, bringing K_M values up or down compared to WT, but the double and triple mutant variants seem to compensate, in comparison, bringing the values within range of WT. A similar trend appears in the k_{cat} values of the peroxidase assays. However, as pH increases, the k_{cat} values of all variants appear to decrease overall compared to WT. There is, however, only a moderate change in peroxidase activity, about 2-fold, when compared to human Cyt*c* which has a 20-40-fold decrease in peroxidase activity.[11] There does not appear to be a trend between the local stability, pK_{app}, and the peroxidase activity of the variants.

The S40T, N63T, V57I, S40T/N63T, V57I/N63T, S40T/V57I and S40T/V57I/N63T variants appear to maintain the local stability of the least stable structures of iso-1-Cyt*c* as indicated by the modest change in pK_{app}. While there is a general decrease in k_{cat} for peroxidase activity for all variants at pH 6 and above, nothing approaching the 20 – 40 fold decrease in peroxidase activity of human Cyt*c* is observed. This observation indicates that there could be interactions of the least stable substructures (Ω-loops C and D) with other more stable substructures of Cyt*c* that modulate the dynamics of these loops that control the k_{cat} of yeast iso-1-Cyt*c*.

References

1. Rajagopal, B., Edzuma, A., Hough, M., et al. (2013) The hydrogen-peroxide-induced radical behaviour in human cytochrome c – phospholipid complexes: implications for the enhanced pro-apoptotic activity of the G41S mutant. *Biochemical Journal* 456(3), 441-452.
2. Hopf, T. A., Ingraham, J. B., Poelwijk, F. J., et al. (2017) Mutation effects predicted from sequence co-variation. *Nature Biotechnology* 35(2), 128-135.
3. Laun, P., Buttner, S., Rinnerthaler, M., Burhans, W. C., and Breitenbach, M., (2012) Aging research in yeast. *Subcellular Biochemistry* 57, 207-232.
4. Huttemann, M., Pecina, P., Rainbolt, M., Sanderson, T. H., Kagan, V. E., Samavati, L., Doan, J. W., Lee, I. (2011) The multiple functions of cytochrome c and their regulation in life and death decisions of the mammalian cell: from respiration to apoptosis. *Mitochondrion* 11(3), 369-381.
5. Kagan, V. E., Tyurin, V. A., Jiang, J., Tyurina, Y. Y., Ritov, V. B., Amscato, A. A., Osipov, A. N., Belikova, N. A., Kapralov, A. A., Kini, V., Vlasova, I. I., Zhao, Q., Zou, M., Di, P., Svitunenko, D. A., Kurnikov, I. V., Borisenko, G. G. (2005) *Nature Chemical Biology* 1, 223-232.
6. Moore, G. R., and Pettigrew, G. W. (1990) Cytochromes c: Evolutionary, Structural and Physicochemical Aspects, Springer-Verlag, New York.
7. Banci, L., Bertini, I., Rosato, A., and Varani, G. (1999) Mitochondrial cytochromes c: a comparative analysis. *JBIC, J. Biol. Inorg. Chem.* 4, 824−837.
8. Alvarez-Paggi, D., Hannibal, L., Castro, M. A., Oviedo-Rouco, S., Demicheli, V., Tortora, V., Tomasina, F., Radi, R., and Murgida, D. H. (2017) *Chem. Rev.* 117(21), 13382-13460
9. Josephs, T. M., Morison, I. M., Day, C. L., Wilbanks, S. M., and Ledgerwood, E. C. (2014) Enhancing the peroxidase activity of cytochrome c by mutation of residue 41: implications for the peroxidase mechanism and cytochrome c release. *Biochem. J.* 458, 259−265.
10. Deacon, O. M., Karsisiotis, A. I., Moreno-Chicano, T., Hough, M. A., Macdonald, C., Blumenschein, T. M. A., Wilson, M. T., Moore, G. R., and Worrall, J. A. R. (2017) *Biochemistry* 56(46), 6111-6124.
11. Nold, S. M., Lei, H., Mou, T., Bowler, B. E. (2017) Effect of a K72A mutation on the structure, stability, dynamics, and peroxidase activity of human cytochrome c. *Biochemistry* 56, 3358-3368.
12. Duncan, M. G., Williams, M. D., and Bowler, B. E. (2009) Compressing the free energy range of substructure stabilities in iso-1-cytochrome c. *Protein Sci.* 18, 1155-1164.